Available online at www.sciencedirect.com
ScienceDirect
Ore Geology Reviews 31 (2007) 261–278
ORE GEOLOGY REVIEWS
www.elsevier.com/locate/oregeorev

Numerical modelling of deformation and fluid flow in the Shuikoushan district, Hunan Province, South China

Yanhua Zhang [a,*], Ge Lin [b], Paul Roberts [a], Alison Ord [a]

[a] *Predictive Mineral Discovery CRC, CSIRO Exploration and Mining, PO Box 1130, Bentley, WA 6102, Australia*
[b] *Key Laboratory of Marginal Sea Geology, Guangzhou Institute of Geochemistry, Chinese Academy of Sciences, Guangzhou 510640, People's Republic of China*

Received 30 November 2003; accepted 16 March 2005
Available online 26 May 2006

Abstract

The Shuikoushan district, in Hunan Province, South China, contains major Pb–Zn–Au–Ag polymetallic mineralisation. Two groups of numerical models have been constructed to study the interactions between deformation and fluid flow in the district during the Yanshanian compression event (180 to 90 Ma). The first group includes district-scale conceptual models of coupled deformation and fluid flow during folding. The models show that fluid flow patterns are controlled by deformation within the fold system inferred for the district. During regional shortening and folding, fluids are generally focused towards the fold hinge/core areas along higher permeability layers (in particular Permian limestone units), in preference to flowing across the low permeability seal units (Permian and Jurassic terrestrial sequences). The efficiency of this fluid focusing can only be significantly increased if these folded seal units are allowed to undergo permeability increase as a result of tensile failure. The modelling results show that permeability enhancement localises mostly at fold hinges, dominantly within the silicified zone on the top of the Permian limestone unit. This process results in increased flow velocities and facilitates fluid focusing towards fold hinge/core locations at this silicified rock horizon. The second group includes deposit scale models for the Kangjiawan deposit, which is one of the two major deposits in the Shuikoushan district. The models show patterns of tensile failure, permeability creation, fluid focusing and mixing, and fracture development along a selected exploration cross section through the deposit. These results are consistent with the observed brecciation and mineralisation features. Regions of maximum brecciation in the district are associated with: (1) a combination of fold hinge and fault intersection locations (structural); and (2) the silicified zone and Permian limestone unit (lithological). Such brecciation zones are associated with extensive fluid focusing and mixing, and therefore represent the most favourable locations for mineralisation in the district. On the basis of this work, ideas for future research work and mineral exploration in the district are proposed.

Keywords: Deformation-fluid flow modelling; Mineralisation; Brecciation; Shuikoushan; South China

1. Introduction

The South China Block is a globally-significant terrane for polymetallic mineralisation, with numerous W, Sn, Mo, Bi, REE, U, Nb, Ta, Pb, Zn, Au, Ag, Cu and Sb deposits known (e.g., Zhuang et al., 1988; Hua and Mao, 1999; Ma, 1999; Pirajno and Bagas, 2002; Li et al., 2002; Pašava et al., 2003; Khin Zaw et al., 2007-this volume). In particular, these (mostly hydrothermal) deposits have a close association with structural processes and magmatic activities during Indosinian–

* Corresponding author. Fax: +61 8 6436 8626.
E-mail address: Yanhua.Zhang@csiro.au (Y. Zhang).

0169-1368/$ - see front matter © 2006 Elsevier B.V. All rights reserved.
doi:10.1016/j.oregeorev.2005.03.013

Yanshanian tectonic events (e.g., Tao et al., 1999; Hua and Mao, 1999; Ma, 1999; Zhou et al., 2002), demonstrating critical tectonic and magmatic controls of mineralisation (e.g., Guo, 1987; Wu, 1994; Yang, 1996; Zhai and Deng, 1996; Pirajno et al., 1997; Zhou et al., 2002; Wang et al., 2002a, 2003a). There have been several summary papers about mineralisation in South China (e.g., Gu et al., 1993; Pirajno and Bagas, 2002; Li et al., 2002; Zhou et al., 2002; Hou et al., 2007-this volume; Chen et al., 2007-this volume; Gu, 2007-this volume) and also a number of studies dealing with specific deposits in the region (e.g., Gu et al., 1992; Pirajno et al., 1997; Jiang and Zhu, 1999; Pašava et al., 2003). Further district-scale detailed studies of key mineralising districts, focusing on structural and/or magmatic controlling factors, are necessary, to advance understanding of mineralisation in South China.

The Shuikoushan district, Hunan Province, is one of the most important mineralised districts within the South China Block (Fig. 1). The region has been an important producer of Pb and Zn in China for over 100 years, and, more recently, has become important in the

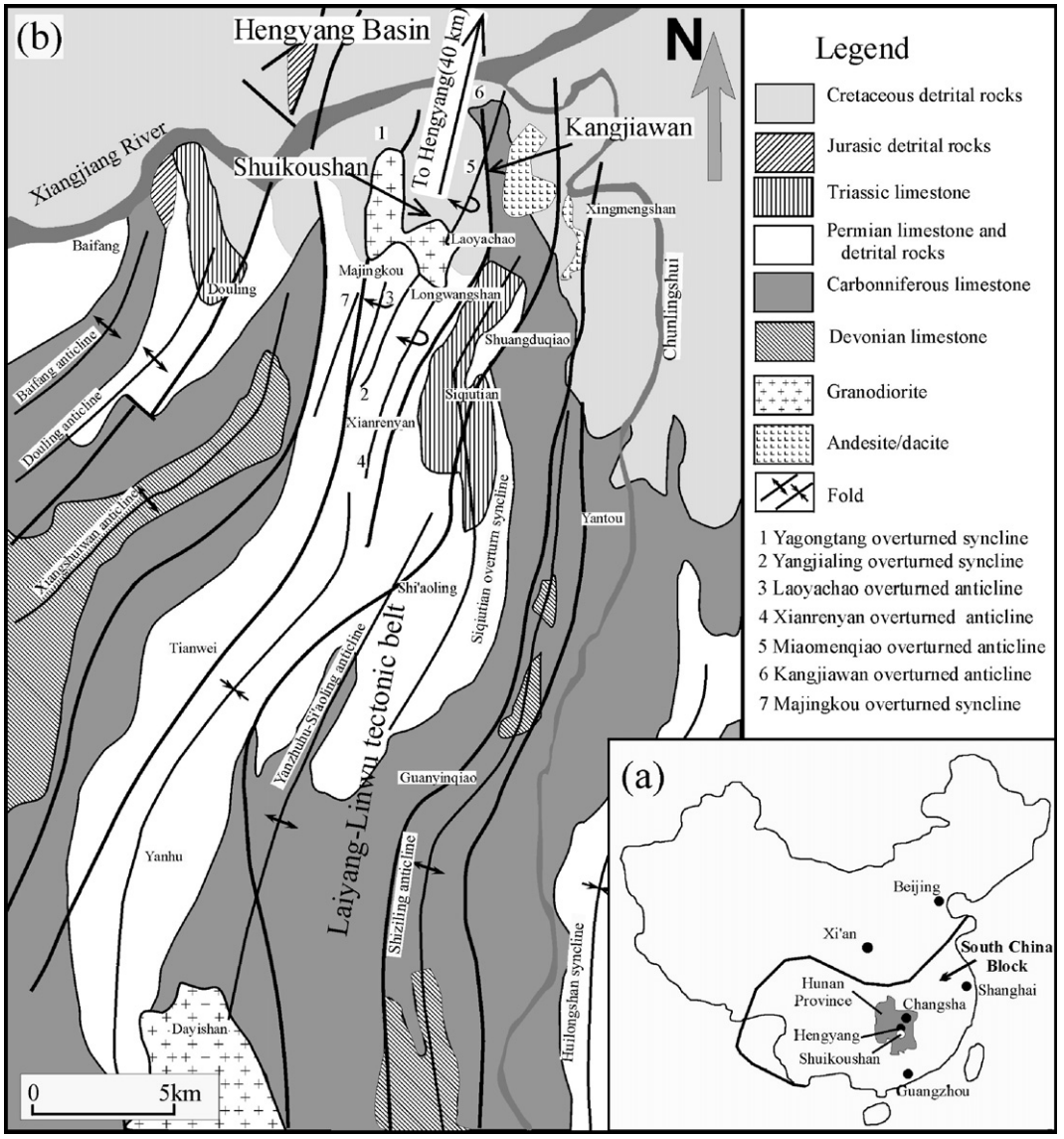

Fig. 1. (a) Location of the Shuikoushan mineralisation district (Hunan Province) within the South China Block. The thick line shows the north–northwest boundary of the South China Block (after Yin and Nie, 1993). (b) Structural outline of the Shuikoushan mineralisation district within the Laiyang–Linwu tectonic belt (adapted from Liu and Tan, 1996b).

production of other metals such as Au, Ag and Cu. Mining operations represent the main industry in the local economy. Because of excellent mineral exploration potential, the district has recently attracted new foreign investment for the exploration of Au.

The Shuikoushan district contains two major deposits, the Kangjiawan Au–Ag–Pb–Zn and the Shuikoushan Pb–Zn–Au–Ag deposits. These are about 2.5 km apart (Fig. 2) and are owned by the Shuikoushan Non-Ferrous Mining Corporation, Limited. The Kangjiawan deposit is currently the most actively mined deposit in the district; exploration of the deposit was completed in 1982 and mining began in 1989. The deposit has total metal contents in excess of 1 MOz Au (Chen et al., 2007-this volume give the grade as 3.65 g/t Au), 0.5 Mt each of Pb and Zn, and 50 MOz Ag. Zeng et al. (2000) indicated that the grade of the ore averages 3.9% Pb, 4.5% Zn, 86.8 g/t Ag and 2.68 g/t Au. The Shuikoushan Pb–Zn–Au–Ag deposit is an old and famous deposit in China. Mining there began in 1896, and its ore reserve is now almost exhausted.

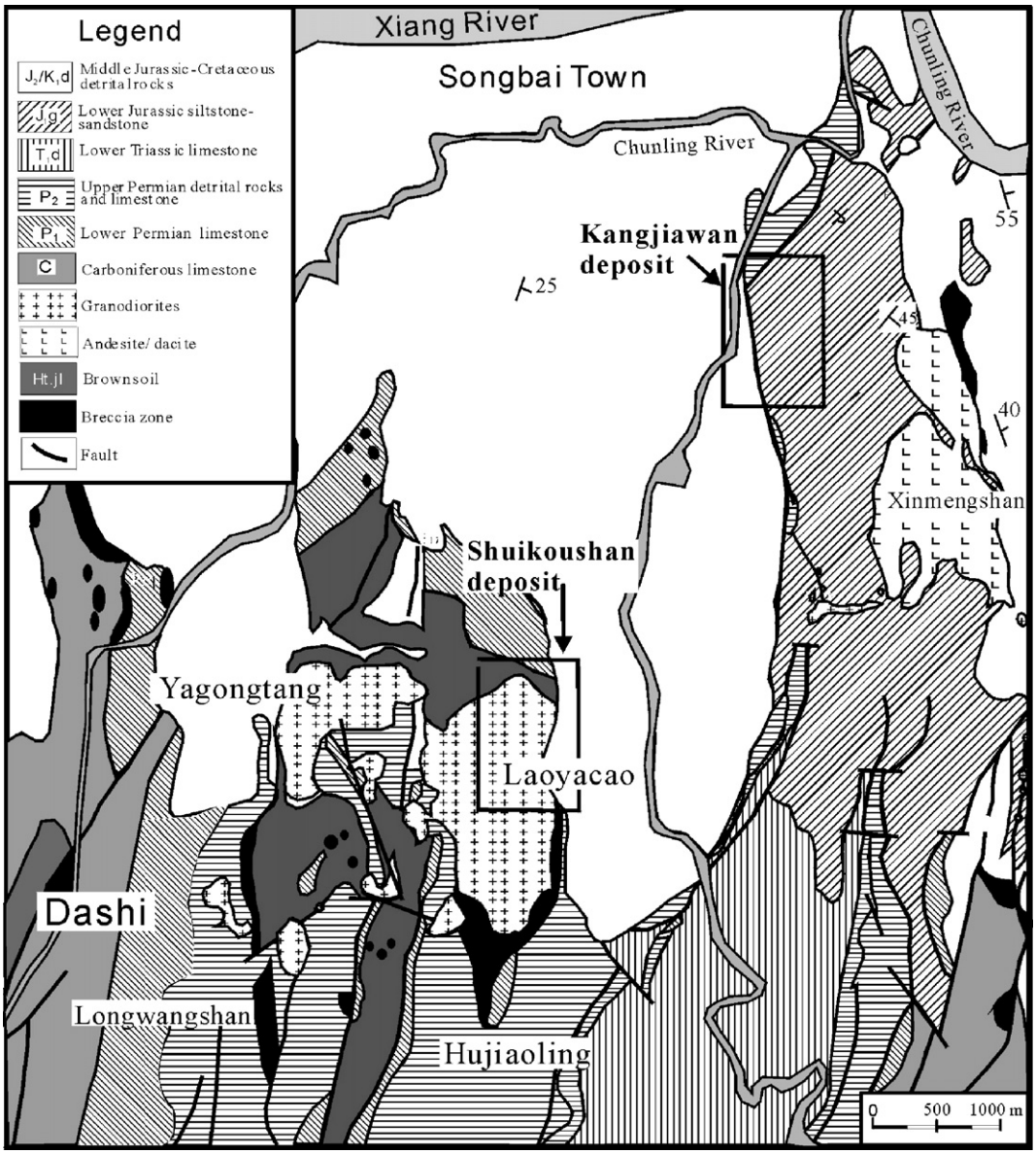

Fig. 2. Geological map of the Shuikoushan mineralisation district, Hunan, China (adapted from Liu and Tan, 1996b).

There have been several studies on mineralisation in the Shuikoushan district. However relevant publications are all in Chinese. A summary description of the features of stratigraphy, magmatic intrusions, structures and ore textures in the Shuikoushan deposit can be found in Zhang (1999), who suggested that the mineralisation is closely associated with intrusive bodies (mainly granodiorite) and is subject to strong structural control (folding, faulting and brecciation) (see also Liu and Tan, 1996a,b). All the other studies are mainly on geochemical features of the deposits. Liu (1994) analysed the geochemistry of fluid inclusions in both the Kangjiawan and the Shuikoushan deposits. He suggested that mineralising fluids were likely derived from the mixing of magmatic fluids with meteoric waters, and that the precipitation of metals was controlled by brecciation structures. Liu and Tan (1996a) simulated chemical reaction and mineral precipitation in the Kangjiawan deposit using a numerical approach, providing information on the chemical evolution of mineralising fluids and the mineral precipitation sequence. Yu and Liu (1997) detailed the lithological and geochemical features of intrusive rocks in the Shuikoushan district and established the genetic relationship between mineralisation and intrusion.

In summary, the previous studies on the Shuikoushan district mostly focused on the geochemical features of the mineralising system, assisted by information from geological observations. These studies have established the following understanding: (1) mineralisation in the district is hydrothermal (see more information in the following section); (2) mineralisation is related to magmatic intrusions and the mineralising fluids are at least partially derived from the intrusive bodies; (3) mineralisation is structurally controlled and occurs mainly at regions of brecciation in folded rocks. However, all the previous studies failed to address the development of rock brecciation and the detailed patterns of fluid flow that evolved during folding in the region. Therefore, this study aims to explore the interaction between deformation and fluid flow associated with mineralisation in the district, using a numerical modelling approach. More specifically, we explore: (1) how rocks deform and brecciation develops in a folding system; (2) how mineralising fluids flow through a multi-layer folded sequence containing impermeable units, and what are the associated fluid flow patterns. Our aim is to generate new understanding of the issues above and to assist future mineral exploration in the district. A brief summary of the current results can also be found in Zhang et al. (2004).

2. Geological background

The Shuikoushan district is located about 40 km south of Hengyang City, Hunan Province, China. Geologically, it is situated at the northern end of the N–S trending Laiyang–Linwu tectonic belt and at the southwestern margin of the Hengyang Cretaceous red-bed basin (Fig. 1b). The geological structures of the district constitute a component of the South China orogenic belt, which is the product of the Indosinian Orogeny (270 to 210 Ma) in combination with the later Yanshanian tectonic event (ca. 180 to 90 Ma) (e.g., Gilder et al., 1996; Pirajno and Bagas, 2002; Wang et al., 2003b, 2005). In a plate tectonics context, the Indosinian event saw the collision between the North China and South China Blocks. The later Yanshanian event, starting from the Early Jurassic, is believed to be related to oblique subduction of the Pacific Plate under the Eurasian Plate along the eastern margin of China. This tectonothermal event led to extensive deformation and magmatic activities in China, in particular, Southeast China. There are, however, recent suggestions that the Yanshanian tectonic–magmatic activities represent an intra-plate deformation event (Chen, 1999; Yan et al., 2003).

The stratigraphic sequence exposed in the district (Fig. 2) consists of Carboniferous limestone–dolomite (C_{1-3}), Permian limestone with a silicified zone at the top (P_{1q} and P_{1d}), a Permian terrestrial sand–silt–clay package (P_{2dl} and P_{2c}; mainly shale with coal seams and marl layers), Triassic limestone with marl and shale layers (T_{1d}), a Jurassic conglomerate–sandstone–muddy siltstone package (J_{1g} and J_2), and Cretaceous sandstone–siltstone–conglomerate rocks (K_{1d}). Two major unconformities separate the Permian/Triassic and Early Jurassic units, and the Cretaceous and Early Jurassic units. There are numerous intrusive bodies exposed in the district but most are small. The only major intrusive body, which has direct contact relationship with the orebodies in the Shuikoushan deposit, is the Shuikoushan granodiorite (exposed in the mine itself). There are no intrusive bodies exposed in the Kangjiawan deposit. There is speculation that mineralisation in Kangjiawan is more distantly related to the granodiorite body (Liu and Tan, 1996a), or that there might be one or more concealed intrusions at depth (Wang, Y.J., personal communication, 2004). Recent U–Pb zircon chronology data (Wang et al., 2002a, 2003a) suggests that the age of the Shuikoushan granodioritic intrusions is ca. 172 Ma, an age consistent with the Yanshanian event.

Fold structures are well developed (Fig. 1b), as a result of the Indosinian and Yanshanian tectonic events.

These are N–S to NNE–SSW trending and form five main anticline–syncline alternating fold systems in the district, all overturned. Faults are also well-developed in the district, mostly along overturned fold limbs. These structures are mostly reverse faults and have dominant N–S to NNE–SSW trends, similar to the fold trends. In some cases, faults are almost bedding parallel. The F_{22} fault in the Kangjiawan deposit and the F_1 fault in the Shuikoushan deposit are the faults most relevant to mineralisation, as demonstrated by the observation that some orebodies are directly hosted within fault zones (Fig. 2; see also Liu and Tan, 1996a).

All the rocks in the district are fractured or brecciated to various degrees. The most severe brecciation is observed in the following three situations: (1) the silicified limestone zone at the top of the Permian limestone unit (P_{1q}), particularly when it intersects with faults and is in unconformable contact with Early Jurassic rocks; (2) the contact zones between the granodiorite intrusive body and the Permian limestone and shale–marl units (P_{1q}, P_{1d}) (Shuikoushan deposit); and (3) near the unconformity below the more rigid Jurassic sandstone.

Ore body–host rock contact relationships differ between the Kangjiawan and Shuikoushan deposits. At Kangjiawan (Figs. 2 and 3), orebodies are mainly hosted in the brecciation zones developed in the silicified section of the Permian limestone (P_{1q}), particularly at intersecting sites between the F_{22} fault, the silicified zone and fold hinge locations (note that the Lower Permian limestone (P_{1q}) is under the cover of the Jurassic–Cretaceous rocks in the area). The breccia zones along the unconformity at the base of the Early Jurassic unit are another favourable ore location, particularly where the silicified limestone zone is in direct contact with the unconformity. Ore bodies are predominantly lens-shaped (Fig. 3), generally 600 to 1200 m long and, on average, 6.8 m thick, and are composed of sulphide ores with massive, disseminated, breccia and fine-vein ore textures. Major ore minerals are galena, sphalerite and pyrite, with a small amount of pyrrhotite, hematite, chalcopyrite, arsenopyrite, bornite and chalcocite.

In the Shuikoushan deposit (Fig. 2), ore bodies are mainly hosted in the breccia contact zones between the granodiorite intrusive body, the Permian limestone (P_{1q}, in particular the silicified zone at the top) and shale–marl unit (P_{1d}), and in faults (e.g., F_1), situated in the core of an overturned anticline. The Permian rocks are also under cover in the deposit. Lens-shaped ore bodies are composed of sulphide ores with dominant massive and breccia ore textures. Major ore minerals are sphalerite, galena, pyrite and chalcopyrite, with a

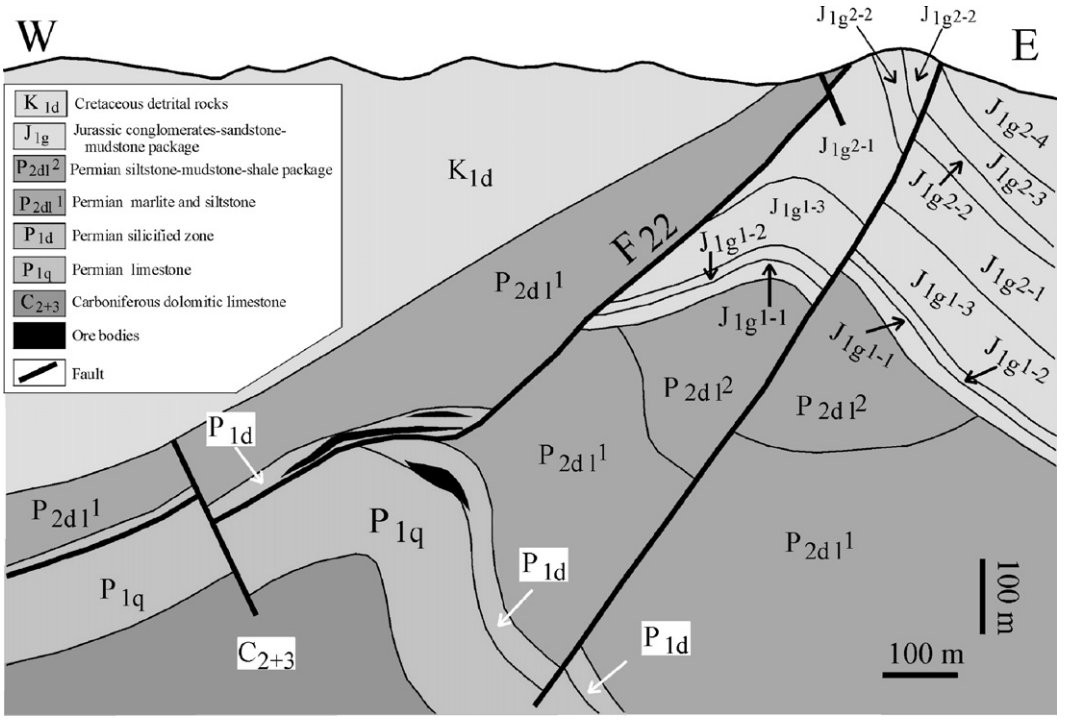

Fig. 3. Structure, stratigraphy and ore body locations in exploration section P104, Kangjiawan Au–Ag–Pb–Zn deposit (based an unpublished exploration profile from the 217 Geological Team of Hunan Geology and Exploration Bureau, China).

small amount of magnetite, hematite, pyrrhotite, scheelite, bismuthinite, molybdenite, bornite, chalcocite, uraninite and stannite.

Previous studies (Liu, 1994; Liu and Tan, 1996a; Yu and Liu, 1997; Zhang, 1999) all suggest that the Kangjiawan and Shuikoushan deposits are genetically linked to the Shuikoushan granodiorite intrusion. The Kangjiawan deposit is described as a hydrothermal replacement deposit involving magmatic and meteoric fluids, while the Shuikoushan deposit is a contact metasomatic skarn deposit involving only magmatic fluids (Liu, 1994; Liu and Tan, 1996a). Mineralisation temperatures in the Kangjiawan deposit (120 to 250 °C) are inferred to be lower than in the Shuikoushan deposit (215 to 430 °C) (Liu and Tan, 1996a). These point to a possible scenario where the migration of magmatic-sourced ore-bearing fluids is from the Shuikoushan intrusion or deposit towards the Kangjiawan deposit. It is then suggested that mineralisation in the Kangjiawan deposit may be somewhat later than in the Shuikoushan deposit (Liu and Tan, 1996a). This scenario is consistent with the fact that the Shuikoushan deposit is in direct contact with the intrusion, while the Kangjiawan deposit is about 2.5 km away from it.

The structural-mineralisation history of the Shuikoushan district is summarised as follows: (1) an early folding/faulting event at approximately 220 Ma, during the Indosinian orogeny, leading to the development of folds and faults and some brecciation in the rock units up to late Triassic; (2) the development of an unconformity, followed by deposition of the Early Jurassic rocks (J_1); (3) the second folding/faulting event from ca. 180 Ma during the early Yanshanian tectonic event, leading to broad/gentle folding of the J_1 rocks, further folding of earlier rock sequences, fault reactivation, and enhanced rock brecciation; (4) granodiorite intrusion at/after about 172 Ma, also within the early Yanshanian event; and (5) mineralisation occurring at, or after, about 172 Ma.

The deformation and fluid flow models in the following sections simulate a part of this history. Our focus is on the interaction between rock deformation, brecciation and fluid flow during the Yanshanian folding/faulting event, immediately before mineralisation in the district.

3. Description of numerical models

3.1. Brief model introduction

We describe here two groups of numerical models, designed to explore the above scenarios. The first group is based on a conceptual district-scale deformation-fluid flow model simulating the coupled deformation-fluid processes during the Yanshanian folding event for the whole Shuikoushan district. The model is not a reconstruction of an actual geological profile, but simulates a conceptual cross section with a synthetic stratigraphic assembly for the district. The second group is at the deposit scale, and focuses on a specific exploration cross section in the Kangjiawan deposit. Furthermore, this group consists of continuum coupled deformation-fluid flow models and a discrete mechanical fracturing model. Details of these models are provided below.

3.2. Modelling technique

A finite difference code, FLAC (Fast Lagrangian Analysis of Continua; Cundall and Board, 1988; Itasca, 1998), has been used in this study to simulate the interactions between deformation and fluid flow. Materials are represented by elements, which form a mesh to fit the geometries of the geological structures to be simulated. Each element behaves according to prescribed mechanical and hydraulic laws in response to the applied boundary conditions. The material can yield and flow, and the grid deforms and moves with the material. This explicit, Lagrangian, computation scheme, together with the mixed-discretisation technique adopted in FLAC, ensure that plastic failure and flow are modelled accurately. This code has previously been successfully applied to the fields of structural geology, tectonics and economic geology (e.g., Hobbs et al., 1990; Ord and Oliver, 1997; Zhang et al., 2000; Ord et al., 2002; Sorjonen-Ward et al., 2002; Wang et al., 2002b; Zhang et al., 2003).

The mechanical behaviour of the model is governed by the Mohr–Coulomb elastic–plastic constitutive law (Jaeger and Cook, 1979, p. 228; Vermeer and de Borst, 1984). A Mohr–Coulomb material undergoing deformation behaves initially elastically until the stress reaches a critical value known as the yield stress, at which point it begins to deform plastically, and irreversibly, to high strain. The yield of such material may be expressed as a yield function, f, given by

$$f = \tau_m + \sigma_m \sin\phi - C\cos\phi,$$

where τ_m is the maximum shear stress and σ_m is the mean stress, ϕ is the friction angle, and C is the cohesion. The material is in an elastic state if $f<0$ (the stress state is not touching the yield surface), and is in a plastic state if $f=0$ (the stress state is touching the

yield surface). The plastic potential function, g, is given by

$$g = \tau_m + \sigma_m \sin\psi - C\cos\psi,$$

where ψ is the dilation angle. The current models adopt $\phi \neq \psi$, resulting in a non-associated flow rule (see Vermeer and de Borst, 1984; Ord, 1991). As a Mohr–Coulomb elastic–plastic material deforms in a plastic manner, it may change in volume. The amount of dilation (plastic volume change) is defined by the dilation angle. On a micro scale, such dilation can be considered as the consequence of the sliding of crystalline grains over one another, or the formation of pore space and fractures (Vermeer and de Borst, 1984; Hobbs et al., 1990; Ord and Oliver, 1997).

Fluid flow in these models is governed by Darcy's Law (see Bear and Verruijt, 1987), given by

$$\boldsymbol{q}_i = -\mathbf{k}^a_{ij}\partial / \partial x_j (P - \rho_w g_k x_k),$$

where $\boldsymbol{q}_i$ is the specific discharge vector or Darcy fluid velocity (m s^{-1}), $\mathbf{k}^a_{ij}$ (m^2) is the apparent mobility matrix, which is a function of permeability and saturation, P is the pressure, ρ_w is the fluid density, g is gravity, and x_i is the position of a material point. Fluid velocities are therefore a function of gradients in pore fluid pressure, or hydraulic head with gravity present, and permeability. Deformation and fluid flow are interactively coupled during modelling. This interaction is reflected in the following ways: (1) pore fluid pressure affects plastic yielding as described in the Mohr–Coulomb yield criteria; (2) volumetric strain developed due to deformation is instantaneously related to fluid pore pressure changes (volume increase or dilation leads to a pore pressure decrease, while volume decrease or contraction results in pore pressure increase); (3) the generation of any topographic elevation or depression, as a result of bulk deformation, can also lead to changes in fluid flow patterns.

The development of a deformation and fluid flow model requires the specification of rock properties relevant to the described rheology including rock density, elastic moduli (bulk modulus and shear modulus), plastic parameters including cohesion, tensile strength, friction angle, and dilation angle, and fluid-related parameters of fluid density, permeability and porosity. Deformation and hydrological boundary conditions (e.g., loading velocity and initial pore pressure) must also be defined.

As a comparative analysis to the continuum approach described above, a discrete-approach model has also been constructed to simulate explicitly the mechanical development of fracture and brecciation, using a finite element code, ELFEN (Rockfield Software Limited, 2001). Similar to the continuum modelling, this discrete model simulates Mohr–Coulomb elastic–plastic rheology but also incorporates a failure law stating that the material will fail in tension and fracture if the maximum tensile stress reaches a critical value.

3.3. Model geometry, mechanical and hydrologic parameters and boundary conditions

The initial geometry of the district-scale fluid flow-folding model consists of 14 stratigraphic units (Fig. 4) and a thin zone associated with the unconformity. The stratigraphy and architecture of the model represents a simplified, conceptual synthesis of the fold structures present in the district before the main mineralisation

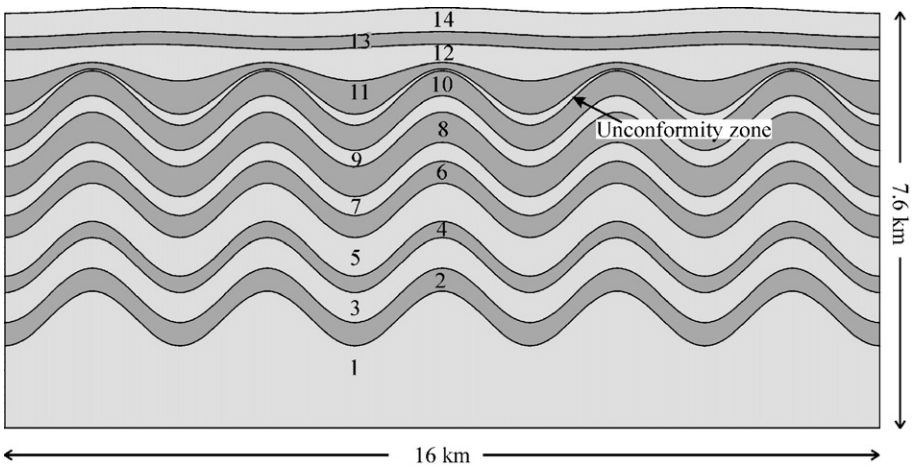

Fig. 4. Initial geometry of the district-scale deformation and fluid flow model. Numbers denote unit no. See Table 1 for the rock types and properties of the units.

Table 1
Mechanical and hydrological properties of the models

Unit no.	Rock types	Period	ρ (kg m^{-3})	K ($\times 10^9$ Pa)	G ($\times 10^9$ Pa)	c ($\times 10^6$ Pa)	σ^t ($\times 10^6$ Pa)	ϕ (°)	k (m^2)
14	Sandstone	Jurassic	2420	33.33	20.0	45.0	22.5	34	3×10^{-16}
13	Mudstone		2350	11.9	8.2	5.0	2.5	25	1×10^{-19}
12	Sandstone		2420	33.33	20.0	45.0	22.5	34	3×10^{-16}
11	Conglomerate		2300	6.17	4.07	10.0	5.0	25	5×10^{-16}
10	Limestone	Triassic	2500	40.0	24.0	50.0	25.0	34	1.5×10^{-16}
9	Calcareous shale		2510	32.05	20.16	42.0	21.0	32	1×10^{-20}
8	Marl with sandy siltstone		2300	24.69	16.26	20.0	10.0	32	1×10^{-17}
7	Siltstone–mudstone–shale with coal seams		2200	13.89	10.42	5.0	2.5	28	1×10^{-19}
6	Marl with sandy siltstone	Permian	2300	24.69	16.26	20.0	10.0	32	1×10^{-17}
5	Silicified zone		2700	75.0	34.62	80.0	40.0	36	1×10^{-18}
4	Limestone		2500	40.0	24.0	50.0	25.0	34	1.5×10^{-16}
3	Dolomitic limestone		2650	49.24	25.39	54.0	27.0	34	2×10^{-16}
2	Limestone	Carboniferous	2500	40.0	24.0	50.0	25.0	34	1.5×10^{-16}
1	Bottom strata		2450	11.1	83.3	10.0	5.0	25	1×10^{-16}
	Unconformity and bedding zones		2100	0.48	0.44	2.0	1.0	15	1×10^{-17}

ρ — density; K — bulk modulus; G — shear modulus; C — cohesion; σ_t tensile strength; ϕ — friction angle; k — permeability; a dilation angle of 2° is used for all the units.

stage, i.e., the second folding event considered to be related to the Yanshanian orogenic period. Since the purpose of the model is to simulate fluid flow patterns during folding rather than fold initiation and development, we have started the model with some existing fold structures, reflecting the framework of the five anticline–syncline fold systems in the district. Note that the pre-Jurassic units (1 to 10) below the major unconformity have tighter folds, reflecting the effects of two folding events (the Indosinian and Yanshanian events), while the units (12 to 14) above the unconformity have much gentler folds, showing the effects of early folding in the second folding event. The models are initialised with a lithostatic pore fluid pressure gradient (Ord and Oliver, 1997) and are subjected to horizontal shortening to simulate further folding and associated fluid flow.

The rock types and mechanical–hydrological properties of the units are given in Table 1. These property values are based on the mechanical characteristics of each rock type, using established data from the literature wherever possible (Clark, 1966; Turcotte and Schubert, 1982). Two scenarios are modelled. In the first scenario, all parameter values are kept constant. In the second scenario, the permeability is allowed to increase when tensile failure occurs, representing permeability change due to deformation mechanisms such as hydrofracturing and brecciation (e.g., Zhang et al., 1999; Zhang and Cox, 2000). This numerical approach to permeability change has been used in several previous studies (e.g., Ord et al., 2002; Sorjonen-Ward et al., 2002).

The deposit-scale cross-section model is based on the structure of the east–west exploration profile (P104) through the Kangjiawan deposit (see Fig. 3); note that this section does not have the complete stratigraphic sequence of the district. The modelling procedure comprises two steps. Firstly, backward geometrical modelling is carried out to recover some shortening

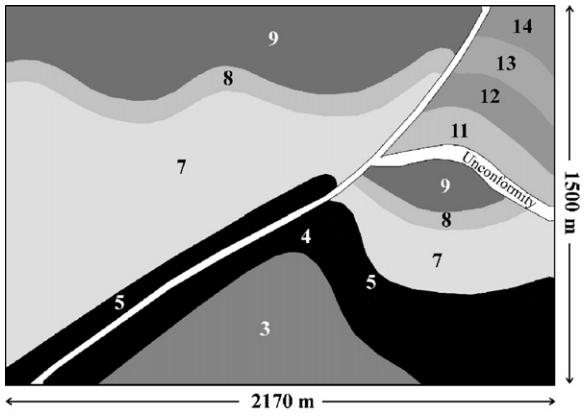

Fig. 5. Reconstructed geometry of structures of the P104 profile in the deposit scale model. See Table 1 for rock types and properties of the units. See text for additional information.

deformation along the profile, based on cross section balancing principles. Secondly, the geometrical structure from the first step (i.e., the pre-mineralisation geometry of the section) is reconstructed for numerical modelling, as shown in Fig. 5. Some simplification has been made for the Jurassic rock units. Stratigraphic unit labelling on the section and relevant rock properties are consistent with those given in Table 1 (also see Fig. 4). The permeability of the F_{22} fault is 2×10^{-15} m^2, the highest in the section. Two different numerical simulations were performed. One is a coupled deformation and fluid flow model using FLAC. The other is a discrete mechanical fracture/brecciation simulation using ELFEN.

4. Modelling results

4.1. Conceptual district-scale deformation-fluid flow model

In the first model (see Fig. 4), fluid flow patterns associated with shortening of a pre-existing fold system are explored for their possible association with mineralisation. The permeabilities assigned to rock units are kept constant throughout the simulation. The model is shortened horizontally by 9% (the simulation stopped for numerical reasons at this stage, because the mesh is locally severely deformed). The deformed geometry, and patterns of shear strain and volumetric strain, are presented in Fig. 6. It is noted that folds in the conceptual profile continued to grow in response to bulk shortening. There are no changes in the number of waveforms, as the initial fold amplitudes are already "finite" and control any further fold amplification (Zhang et al., 1996, 2000). The fold trains in the rock sequences below the unconformity become tighter with steeper fold limbs, and the folds in the Jurassic rocks above the unconformity still exhibit broad fold geometry with gently-dipping limbs. The distribution of shear strain in the folded sequences is inhomogeneous. There is shear strain localisation along bedding planes, particular at fold limbs, reflecting intensive layer-parallel shearing during folding (Hobbs et al., 2000a). This is consistent with the observation that severe deformation (fracturing, brecciation and foliation) occurs along bedding, and some small faults develop along bedding. Volumetric strain distribution is also inhomogeneous. It is noted that there is widespread volume increase or dilation in the system, a consequence of the buckling process. High dilation is predominantly localised at fold hinges, as a result of differential buckling between different units, and also along bedding at fold limbs as a consequence of shear deformation (Ord and Oliver, 1997).

Darcy fluid flow velocities in the central part of the model are given in Fig. 7. The fluid flow field is dominated by intra-layer, bedding parallel flow, with strong fluid focusing into fold hinge areas. We note that fluid flow in this multi-layer fold system is essentially isolated. The main flow is confined to the aquifer units of limestone, dolomitic limestone, conglomerates and sandstone, while several other units (shale, mudstone and siltstone) act as "seals" and show little fluid flow. Fluid flow rates in the system are very slow, as indicated by the maximum fluid flow rate of 1.94×10^{-9} m s^{-1}. Folding leads to the development of some low topographic relief near the surface, and this generates downward fluid flow, potentially representing the input of meteoric water. However, such flow is confined to the top sandstone unit, because of the presence of a mudstone seal unit underneath. All these features show that the fluid flow field for the model represents a very inefficient system for mineralisation.

The assumption of constant permeability can be problematic, because there are several deformation-related mechanisms (e.g., hydrofracturing, brecciation and grain size/compaction changes), which can change rock permeability in nature. In the next model, we explore the effect of deformation-enhanced permeability on fluid flow patterns, by incorporating an algorithm that causes the permeability of rock units to increase to a value of 2×10^{-15} m^2 when the material fails in tension. The high permeability distribution and Darcy fluid flow velocities for the central region of the model at 9% shortening is illustrated in Fig. 8. The results show that tensile failure and permeability enhancement mainly occur at fold hinges (or fold core regions in a multi-layer folding systems) and limbs. Most of the low-permeability units (e.g., unit 5 — the silicified limestone unit in particular) are breached with the development of high permeability zones (representing fracturing/brecciation). The above results in a much more efficient flow field where fluids can be transported across low permeability units for a longer distance and focus into fold hinge/core areas. Fluid flow velocities, with a maximum rate of 2.142×10^{-8} m s^{-1}, are also much greater than those in the previous (constant permeability) model. There seems to be two types of locations for significant fluid focusing. The first includes fold hinge/core locations in the silicified zone plus limestone and dolomitic limestone rocks (units 2 to 4 and unit 5 in the tensile failure/fractured state) below the relatively low-permeability units (6 to 9) of the siltstone–mudstone–shale–marl package. The second includes fold hinge/core locations of units 9 to 11 beneath the unconformity zone. These features are consistent with the ore

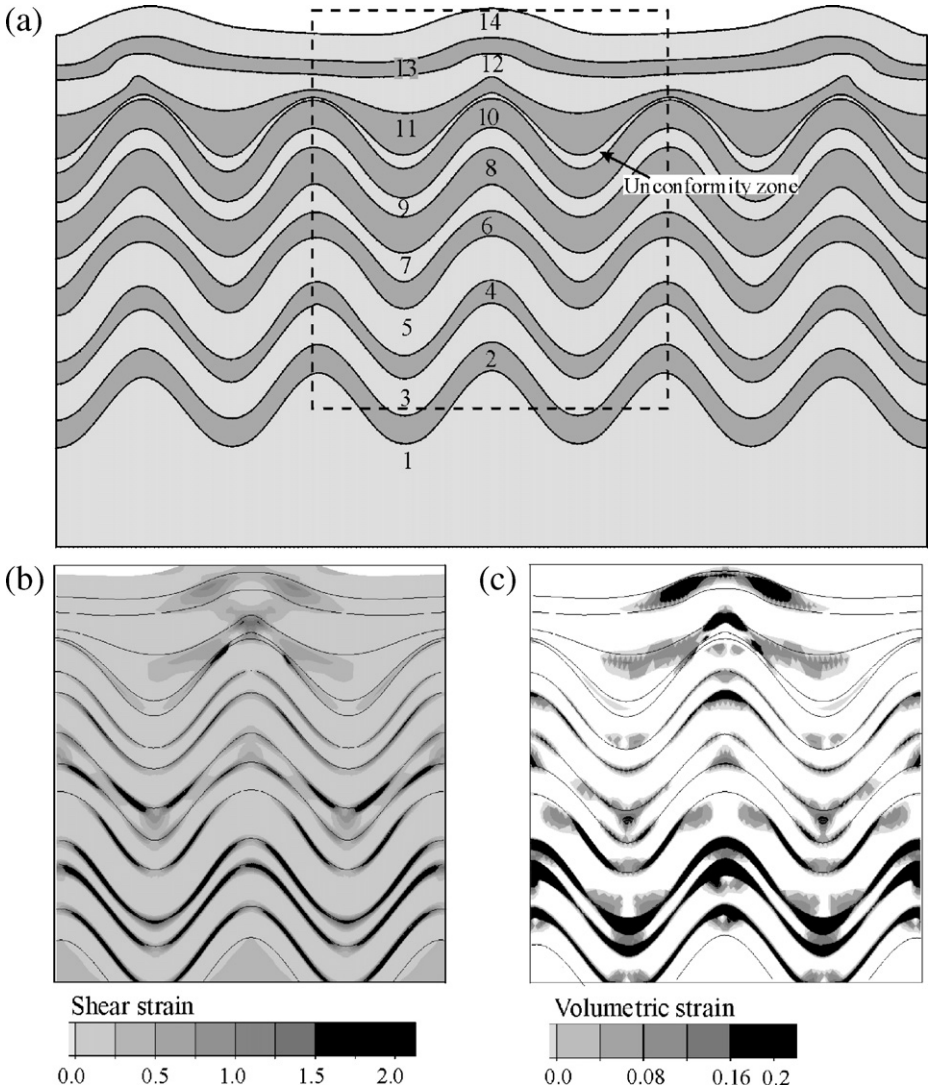

Fig. 6. Deformed fold geometry of the district-scale deformation-fluid flow model at 9% bulk shortening (a). The dash-line box defines the area for illustrating distributions of shear strain (b) and of volumetric strain (dilation) (c). See Table 1 for the rock types and properties of the units.

positions observed in both the Kangjiawan deposit and the Shuikoushan deposit. It is also noted that downward fluid flow associated with low topographic relief at the surface penetrates the mudstone seal layer (unit 14) and reaches deeper sequences. This would potentially facilitate influx of meteoric water and fluid mixing, a scenario suggested by Liu (1994) based on the geochemical characteristics of fluid inclusions.

4.2. Deposit-scale deformation and fluid flow model

The deposit-scale model (see Figs. 3 and 5) for the exploration cross section P104 in the Kangjiawan Au–Ag–Pb–Zn deposit uses the same mechanical and hydrological properties and rock unit sequence numbers as the district scale models (Table 1). In addition, the model incorporates the structure of a fault (F_{22}). The fault has the following properties: density = 2100 kg m^{-3}, bulk modulus = 1.666×10^{10} Pa, shear modulus = 1.25×10^{10} Pa, cohesion = 1×10^{7} Pa, tensile strength = 0.5×10^{7} Pa, friction angle = 25° and permeability = 2×10^{-15} m^2. A lithostatic initial fluid pore pressure gradient is adopted. As in the models described above, we have incorporated an algorithm that allows the permeabilities of rock units to increase to 2×10^{-15} m^2 when materials fail in tension. The model is horizontally shortened by about 5%. The locations of tensile failure, the developed high permeabilities and Darcy fluid flow

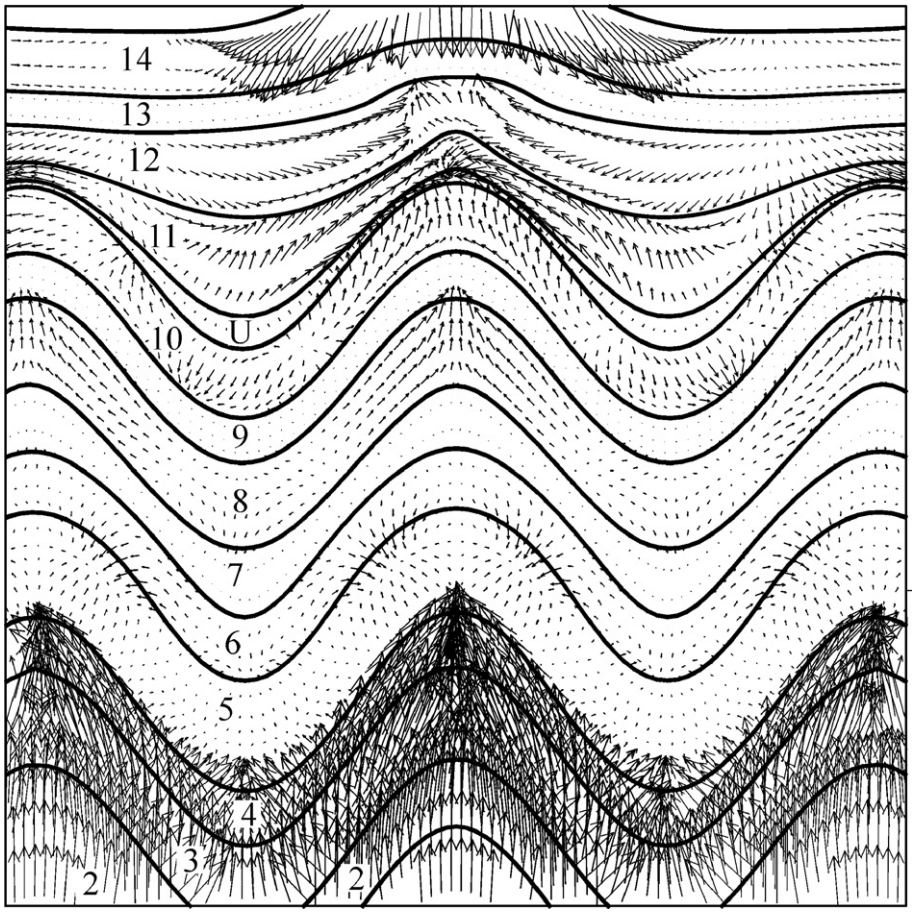

Fig. 7. Instantaneous Darcy fluid flow velocities in the central area of the district-scale model (see the dash-line box in Fig. 5a) at about 9% bulk shortening. See Table 1 for the rock types and properties of the units; "U" denotes the unconformity zone. Permeability is kept constant in the model. The maximum fluid flow rate is 1.99e-9 m s^{-1}.

velocities for the central area of the model are shown in Fig. 9. It is interesting to note that tensile failure (effectively representing brecciation) and high permeability creation are dominantly localised in the fold hinge/core area where the silicified zone and limestone intersect with the F_{22} fault. The overturned limb of the fold (the silicified zone and limestone units) also seems to show more tensile failure and associated permeability creation. As a result of tensile failure and permeability creation, fluids are strongly focused towards these locations. In the meantime, some downward fluid flow along the F_{22} fault is also directed towards these locations. Such fluid flow patterns create an ideal scenario for fluid mixing, favourable for mineralisation (Hobbs et al., 2000b; Zhang et al., 2003). Furthermore, the pattern of fluid mixing predicted by this model explicitly replicates the conceptual fluid mixing scenario of Liu (1994) for the Shuikoushan district.

The results from the model above are generally consistent with the observations of rock brecciation and ore body distributions in the cross section through the Kangjiawan deposit. Underground observations, however, indicate that the silicified zone on the top of the limestone unit seems to be more severely brecciated than the limestone unit, while the silicified zone in the model shows relatively less tensile failure. This is probably due to the high tensile strength of 4×10^7 Pa used for the unit in the model (the highest value of the model, see Table 1). The rocks in the silicified zone are actually very brittle, and should have higher cohesion (as used in the model) and lower tensile strength. To explore this scenario, we have constructed another model with the modification of tensile strength from 4×10^7 to 1×10^7 Pa.

The resulting tensile failure locations, high permeability creation and Darcy fluid flow velocities for the modified model are presented in Fig. 10. It can be seen

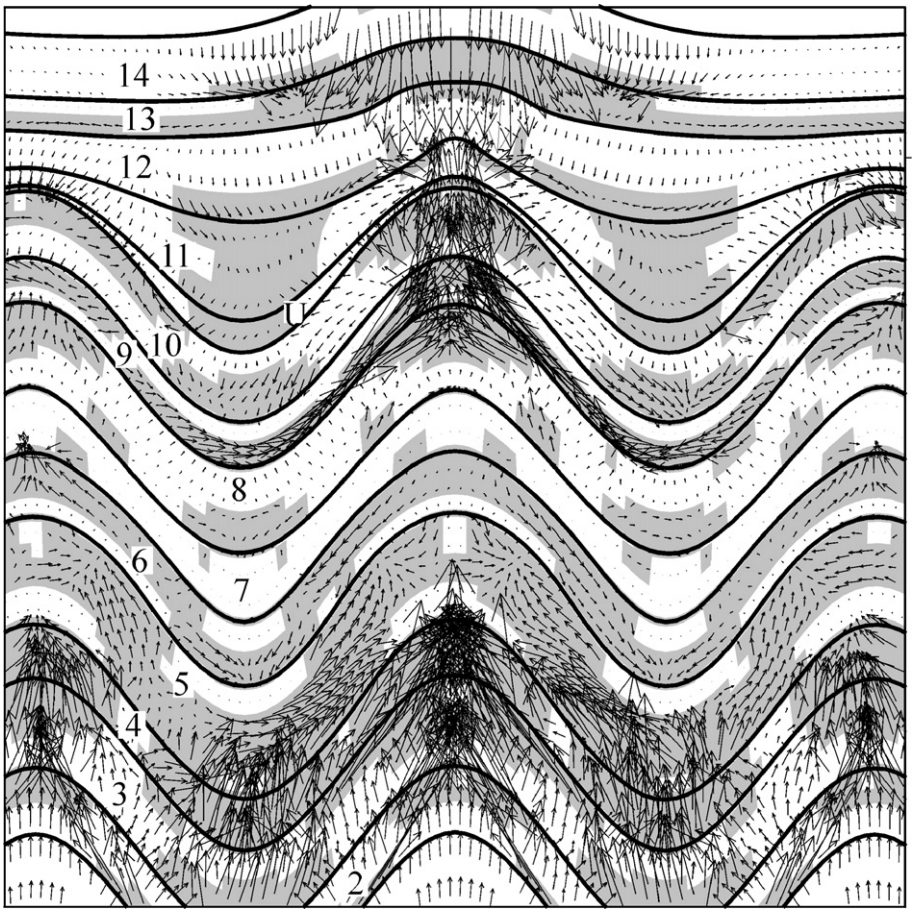

Fig. 8. Instantaneous Darcy fluid flow velocities in the central area of the district-scale model (see the dash-line box in Fig. 5a) at about 9% bulk shortening. See Table 1 for the rock types and properties of the units; "U" denotes the unconformity zone. Permeability is allowed to increase when tensile failure occurs. Shaded areas indicate the locations of permeability enhancement as a result of tensile failure. The maximum fluid flow rate is 2.14e-8 m s^{-1}.

that the area of tensile failure in the silicified unit became more extensive. The rocks at the fold hinge and overturned-limb locations have failed extensively. The limestone unit underneath also shows extensive tensile failure. These features are consistent with the observation of severe fracturing — brecciation and mineralisation at the corresponding structural location in the Kangjiawan deposit. The fluid flow pattern is consistent with that described for the previous model, that is, strong fluid focusing (maximum rate = 1.67×10^{-7} m s^{-1}) and mixing at the fold hinge location or the "brecciated" areas within the silicified zone and limestone unit, where the F_{22} fault cuts through.

We note that there are also some other small areas showing tensile failure and permeability increase (see Figs. 9 and 10). But fluid flow at these locations is insignificant because these small high permeability areas are isolated.

4.3. Deposit-scale discrete fracture-brecciation model

The Elfen discrete fracture-brecciation model for the P104 profile uses properties consistent with those used in the FLAC continuum approach modelling described above. The model uses a low tensile strength for the silicified unit, and is also subject to horizontal shortening. It is interesting to note that fracture development in the model is remarkably consistent with the pattern of tensile failure predicted by the continuum deformation-fluid flow models (Fig. 11; also see Figs. 9 and 10) and coincides well with ore body locations on the P104 exploration profile in the Kangjiawan deposit. Extensive fractures develop in the silicified zone and limestone unit, but are predominantly confined to the fold hinge location; fracturing in the other areas of the model is minimal. This is consistent with the observation of severe rock

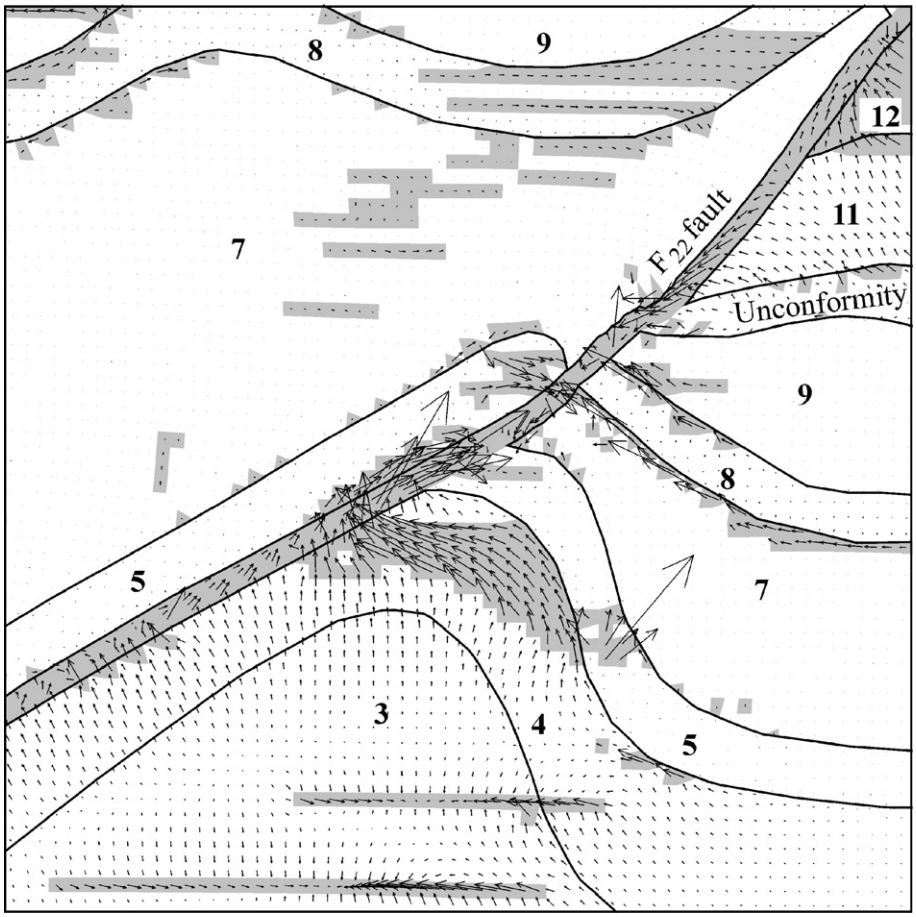

Fig. 9. Instantaneous Darcy fluid flow velocities in the central area of the deposit-scale model for the P105 profile in the Kangjiawan deposit at about 5% bulk shortening. See Table 1 for the rock types and properties of the units. Shaded areas indicate the locations of permeability enhancement as a result of tensile failure. The maximum fluid flow rate is 2.15e-7 m s^{-1}.

brecciation and mineralisation at such locations in the Kangjiawan deposit.

5. Discussion

In the Shuikoushan district, brecciation has been considered the most important mechanical control on mineralisation sites, based for example on the occurrence of ore bodies in the breccia zones along the silicified zone of the Permian limestone in the Kangjiawan deposit. Except for some general descriptions of brecciation features and locations (e.g., Liu, 1994; Liu and Tan, 1996a; Zhang, 1999), there is no detailed discussion of the development of breccias in the district. The current models have, for the first time, explored the folding and fluid flow process, showing how brecciation could have developed as a consequence of folding and faulting. Our results show that tensile failure and fracturing were the most likely processes controlling the brecciation. These effects are closely related to the pore fluid pressure gradient (high fluid pressures facilitate brecciation; see Sorjonen-Ward et al., 2002), the mechanical properties (for example, high cohesion and low tensile strength, i.e., more brittle rock which is easier to brecciate), and structural locations (e.g., fold hinge, limb and fault intersections). In the Shuikoushan district, the silicified zone together with the underlying Permian limestone unit represent the lithological control on brecciation; and the fold hinges and limbs (especially when overturned) represent the structural control, particularly where these locations intersect with major faults. This understanding is also consistent with observations of brecciation or fracture-related vein structures in many other mineral deposits in the world (e.g., Schaubs and Zhao, 2002; Ord et al., 2002; Potma et al., 2003).

Fluid flow in folded systems is an important issue relevant to mineralisation in many regions (e.g., Ord et

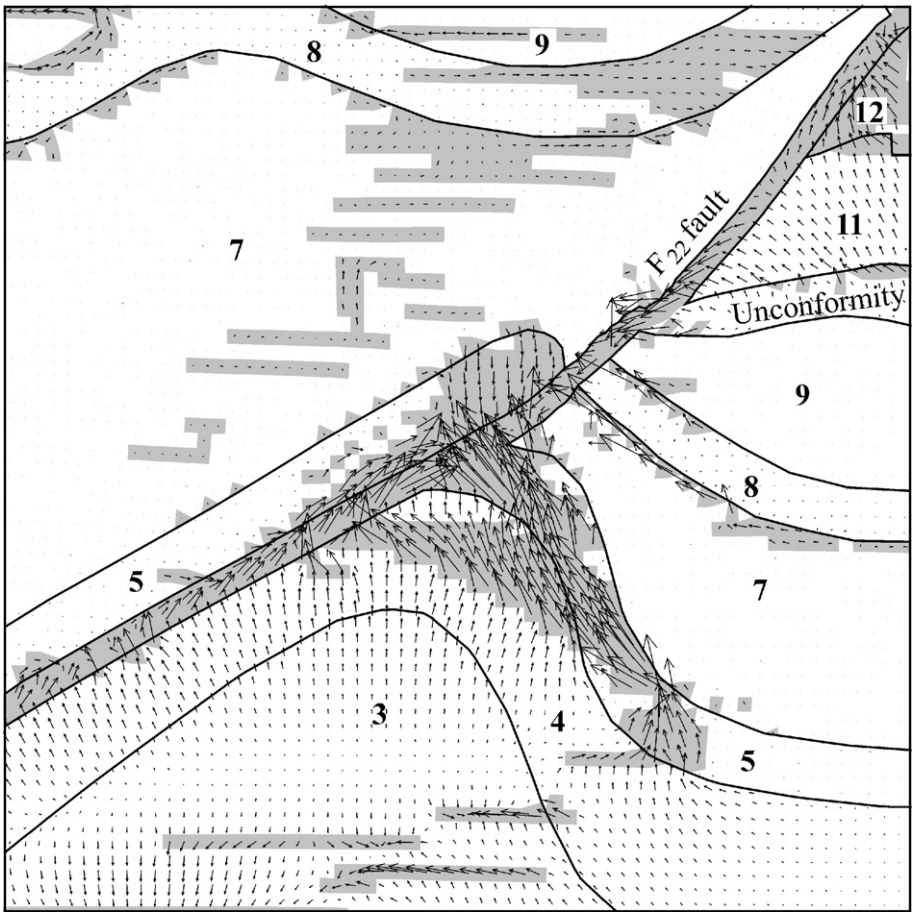

Fig. 10. Instantaneous Darcy fluid flow velocities in the central area of the deposit-scale model for the P105 profile in the Kangjiawan deposit at about 5% bulk shortening. This model uses a lower tensile strength for the silicified zone than the previous model (see text for detailed description). See Table 1 for the rock types and properties of the units. Shaded areas indicate the locations of permeability enhancement as a result of tensile failure. The maximum fluid flow rate is 1.67e-7 m s^{-1}.

al., 2002). For the Shuikoushan district, the general perception of previous workers (e.g., Liu, 1994; Yu and Liu, 1997; Zhang, 1999) is that fluids would flow predominantly upward from the fluid source (one or more intrusions) to mineralizing sites in the system. However, folds in the district involve a complex stratigraphic assembly ranging from very impermeable rock types (shale, mudstone and siltstone) to more permeable lithologies (sandstone, conglomerates and limestone). The presence of low permeability layers will tend to limit fluid transport in the system. These results show that the fluid flow regime in the Shuikoushan district would have been characterised by inefficient, isolated, intra-bed flow if the permeabilities of rock units did not change with deformation. In nature, however, permeabilities did change with deformation, particularly as a result of tensile failure. The results presented in this study show intense, localised shearing on fold limbs, dilation in fold hinges, and tensile fracturing of the more brittle rocks in regions of high pressure and buckling-related tensile, or low minimum principal, stresses. These processes led to the creation of high permeability in the system and the breaching of low permeability "seal" units. As a result of these coupled processes, fluid flow in the system became connected and more efficient, enabling transport of fluids through the multi-layer package and fluid focusing into fold hinge/core locations.

Fluid mixing and the involvement of meteoric waters in the mineralising fluids for the district, proposed by Liu (1994), is a likely scenario. The current results show that low topographic relief, generated by folding, promoted the downward flow of meteoric water, assisted by the breaching of "seal" units. Furthermore, the cross section model clearly demonstrates that, in addition to pervasive flow through rock sequences

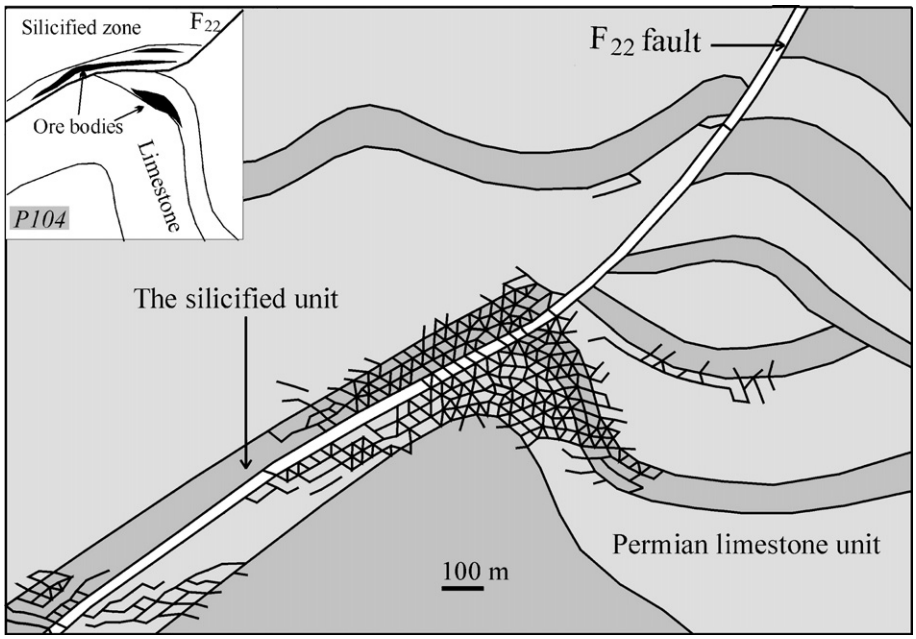

Fig. 11. Brecciation pattern developed in the deposit-scale discrete fracture-brecciation model. Short black lines/mesh illustrate the fracture geometry. Ore body locations on the P104 exploration profile in the Kangjiawan deposit are illustrated in the diagram inset at top-left (see Fig. 3 for details).

(assisted by rock tensile failure and permeability creation), fluids also migrated upward (deep levels) and downward (shallower levels) preferentially along the F_{22} fault. Such fluid flow patterns promoted the development of fluid mixing sites in the fold hinge area (see Figs. 9 and 10). Therefore, the role of major faults in transporting fluids during mineralisation in the district was critical. This role is consistent with the understanding of the relationship between faults and fluid flow (e.g., Knipe, 1993; Sibson, 1994; Oliver, 1996; Zhang et al., 2003).

It has been widely recognised that numerous polymetallic deposits in the South China Block are genetically related to the Yanshanian tectono-magmatic event from ca. 180 to 90 Ma (e.g., Guo, 1987; Wu, 1994; Yang, 1996; Zhai and Deng, 1996; Pirajno et al., 1997; Hua and Mao, 1999; Tao et al., 1999; Zhou et al., 2002). Extensive magmatic activity and structural reworking over the period provided excellent conditions for the evolution and transport of mineralising hydrothermal fluids. As such, South China still represents a highly prospective terrain for mineral exploration as demonstrated by increased exploration activity in recent years. However, it needs to be recognised that mineralisation conditions (structural and thermal) during the Yanshanian period can be very different from region to region within South China. For example, Hunan Province (the most important polymetallic province in South China) consists of several broad polymetallic zones, each with different mineralisation temperatures (from low to high temperature mineralisation) and different mineral assemblages. The Shuikoushan district is located in the intermediate temperature ore belt of this system. The development of such lateral mineralisation temperature gradients may have been the result of several different tectonic processes, such as magmatic underplating, crustal scale thrusting and broad crustal thickening. Careful research is needed to discriminate these scenarios. The preliminary work of Zhang et al. (2004) has already highlighted the important role of crustal thrusting in the development of lateral geothermal gradients. The work of Wang et al. (2002b) also described the role of thrusting and related inhomogeneous crustal thickening in the formation of granites in South China.

6. Conclusions

Coupled district-scale deformation-fluid flow models show that fluid flow patterns for the fold system inferred for this region were controlled by deformation within fold structures. Fluids were generally focused towards the fold hinge/core areas. Fluids flow along higher permeability layers towards the hinges in preference to flowing across the low permeability seal units. The efficiency of the system was probably significantly

increased where folded rock units experienced permeability increases as a result of tensile failure. These results show that new permeability development localised mostly at fold hinges, dominantly within the silicified zone on the top of the Permian limestone unit. This process resulted in increased flow velocities and facilitated fluid focusing towards fold hinge/core locations.

The deposit scale cross-section models predict the patterns of tensile failure, permeability creation, fluid focusing and mixing, and fracture development. These predictions explain brecciation and mineralisation features observed on a selected profile. Locations of brecciation in the district are characterised by: (1) combination of fold hinge and fault intersection locations (structural) and (2) the silicified zone and limestone unit (lithological). Such brecciation zones are associated with extensive fluid focusing and mixing, and therefore represent the most favourable locations for mineralisation in the district.

Based on these results, future exploration in the district should focus on identifying the locations where the silicified zone and the Permian limestone package is folded and intersected by major F_{22}-like faults, and is covered by a low permeability terrestrial sand–silt–clay sequence (seal). The presence of intrusive bodies in near-by areas or at deeper levels will increase the probability of mineralisation. On this basis, the south margin of the Hengyang basin and the regions south of the Shuikoushan district (the central part of the Laiyang–Linwu tectonic belt) appear to be prospective and deserve more attention (see Fig. 1b). Furthermore, detailed geophysical work to establish the locations and geometries of concealed intrusive bodies and further detailed structural–geophysical work to establish the 3D structural architecture of the district will enhance the possibility of success in mineral exploration in the district in the future.

Acknowledgements

The authors would like to thank Nigel Cook and an anonymous reviewer for their critical and constructive comments, which resulted in major improvements to the manuscript. Heather Sheldon, Warren Potma and Wang Yuejun are thanked for reading, correcting and commenting on earlier versions of the manuscript. We are also grateful to Wang Yuejun and Guanghao Chen at Guangzhou Institute of Geochemistry, Greg Hall at Placer Dome Inc., Yunqi Pang and Zhongyan Tan at the Shuikoushan Non-Ferrous Mining Corp., and Kaixuan Tan at Nan-Hua University for their advice and assistance during this work. Financial support from the Chinese National Fund of Science (grant no. 40334039), the Chinese Academy of Sciences (grant no. GIGCX-03-02), the Predictive Mineral Discovery Cooperative Research Centre, and the Australia–China Special Cooperation Fund for Scientific and Technological Cooperation is gratefully acknowledged. Special thanks are due to Khin Zaw for his support and encouragement to publish this paper and editorial handling of the manuscript.

References

Bear, J., Verruijt, A., 1987. Modelling Groundwater Flow and Pollution. D. Reidel, Dordrecht. 414 pp.

Chen, A., 1999. Mirror thrusting in the South China Orogenic belt: tectonic evidence from western Fujian, southeastern China. Tectonophysics 305, 497–519.

Chen, Y., Chen, H.Y., Khin Zaw, Pirajno, F., Zhang, Z.J., 2007. Geodynamic setting and tectonic model of skarn gold deposits in China—an overview. Ore Geology Reviews 31, 139–169 (this volume). doi:10.1016/j.oregeorev.2005.01.001.

Clark Jr., S.P. (Ed.), 1966. Handbook of Physical Constants. Geological Society of America Memoir, vol. 97. New York. 587 pp.

Cundall, P.A., Board, M., 1988. A microcomputer program for modelling large-strain plasticity problems. In: Swoboda, G. (Ed.), Proceedings of the Sixth International Conference on Numerical Methods in Geomechanics. Numerical Methods in Geomechanics, vol. 6, pp. 2101–2108.

Gilder, S.A., Gill, J., Coe, R.S., Zhao, X.X., Liu, Z.W., Wang, G.X., 1996. Isotopic and paleomagnetic constraints on the Mesozoic tectonic evolution of South China. Journal of Geophysical Research, B 107, 16137–16154.

Gu, L.X., Yang, H., Zheng, S., Liao, J.G., 1992. Tungsten enrichment in the South China-type massive sulphide deposits. Chinese Journal of Geochemistry 11, 344–351.

Gu, L.X., Hu, W., He, J.X., Xu, Y.T., 1993. Geology and genesis of Upper Palaeozoic massive sulphide deposits of South China. Transactions of the Institution of Mining and Metallurgy, Section B: Applied Earth Science 102, B83–B96.

Gu, L., Hu, W., Pi, N., Khin Zaw, He, J., 2007. Peculiar features of Upper Palaeozoic massive sulphide deposits in South China. Ore Geology Reviews 31, 107–138 (this volume). doi:10.1016/j.oregeorev.2005.01.002.

Guo, W., 1987. Guide to the metallogenic map of endogenic ore deposit of China (1:4,000,000). Cartographic Publishing House, Beijing.

Hobbs, B.E., Mühlhaus, H.-B., Ord, A., 1990. Instability, softening and localisation of deformation. In: Knipe, R.J., Rutter, E.H. (Eds.), Deformation Mechanisms, Rheology and Tectonics. Geological Society of London Special Publication, vol. 54, pp. 143–165.

Hobbs, B.E., Mühlhaus, H.-B., Ord, A., Zhang, Y., Moresi, L., 2000a. Fold geometry and constitutive behaviour. In: Jessell, M.W., Urai, J.L. (Eds.), Stress, Strain and Structure. Journal of the Virtual Explorer. paper 19 (printed abstract with full text on a CD). http://www.virtualexplorer.com.au.

Hobbs, B.E., Ord, A., Archibald, N.J., Walshe, J.L., Zhang, Y., Brown, M., Zhao, C., 2000b. Geodynamic modelling as an exploration

tool. After 2000 — The Future of Mining, AusIMM Annual Conference Proceedings 2000, Melbourne, pp. 34–48.

Hou, Z., Khin Zaw, Pan, G., Xu, Q., Hu, Y., Li, X., 2007. Sanjiang Tethyan metallogenesis in S.W. China: tectonic setting, metallogenic epochs and deposit types. Ore Geology Reviews 31, 48–87 (this volume). doi:10.1016/j.oregeorev.2004.12.007.

Hua, R.M., Mao, J.W., 1999. A preliminary discussion on the Mesozoic in east China. Mineral Deposits 18, 300–308 (in Chinese with English abstract).

Itasca, 1998. FLAC: Fast Lagrangian Analysis of Continua, User Manual, Version 3.4. Itasca Consulting Group, Inc., Minneapolis.

Jaeger, J.C., Cook, N.G.W., 1979. Fundamentals of Rock Mechanics, 3rd Edition. Chapman and Hall, London. 593 pp.

Jiang, N., Zhu, Y.F., 1999. Geology and genesis of orogenic gold deposits, Xiaoqinling district, southeastern China. International Geology Review 41, 816–826.

Khin Zaw, Peters, S.G., Cromie, P., 2007. Nature, diversity of deposit types and metallogenic relations of South China. Ore Geology Reviews 31, 48–87 (this volume). doi:10.1016/j.oregeorev.2005.10.006.

Knipe, R.J., 1993. The influence of fault zone processes and diagenesis on fluid flow. In: Horbury, A.D., Robinson, A.G. (Eds.), Diagenesis and Basin Development. American Association of Petroleum Geologists, Studies in Geology, vol. 36, pp. 135–154.

Li, J.W., Zhou, M.F., Li, X.F., Fu, Z.R., Li, Z.J., 2002. Structural control on uranium mineralisation in South China: implications for fluid flow in continental strike-slip faults. Science in China, Series D: Earth Sciences 45, 851–864.

Liu, W., 1994. Nature, source and convection path of the ore-bearing fluid in the Shuikoushan Pb–Zn–Au ore field. Geotectonica et Metallogenia 18, 209–218 (in Chinese with English abstract).

Liu, S., Tan, K., 1996a. Dynamics of tectonic ore-forming in open system in Shuikoushan ore field, Hunan. Geotectonica et Metallogenia 20, 1–9 (in Chinese with English abstract).

Liu, S., Tan, K., 1996b. Dynamics of Ore-forming in Open Systems: the Mechanism of Ore-forming of the Shuikoushan Ore Field. Seismological Press, Beijing. 112 pp., (in Chinese with English abstract).

Ma, D.S., 1999. Regional pattern of element composition and fluid character in medium-low temperature metallogenic province of South China. Mineral Deposits 18, 347–358 (in Chinese with English abstract).

Oliver, N.H.S., 1996. Review and classification of structural controls on fluid flow during regional metamorphism. Journal of Metamorphic Geology 14, 477–492.

Ord, A., 1991. Deformation of rock: a pressure-sensitive, dilatant material. Pure and Applied Geophysics 137, 337–366.

Ord, A., Oliver, N.H.S., 1997. Mechanical controls on fluid flow during regional metamorphism: some numerical models. Journal of Metamorphic Geology 15, 345–359.

Ord, A., Hobbs, B.E., Zhang, Y., Broadbent, G.C., Brown, M., Willetts, G., Sorjonen-Ward, P., Walshe, J.L., Zhao, C., 2002. Geodynamic modelling of the Century deposit, Mt Isa Province, Queensland. Australian Journal of Earth Sciences 49, 935–964.

Pašava, J., Kříbek, B., Dobeš, P., Vavřín, I., Žák, K., Delian, Fan, Tao, Zhang, Boiron, M.C., 2003. Tin–polymetallic sulphide deposits in the eastern part of the Dachang tin field (South China) and the role of black shales in their origin. Mineralium Deposita 38, 39–66.

Pirajno, F., Bagas, L., 2002. Gold and silver metallogeny of the South China Fold Belt: a consequence of multiple mineralizing events? Ore Geology Reviews 20, 109–126.

Pirajno, F., Bagas, L., Hickman, A.H., Gold Research Team, 1997. Gold mineralisation of the Chencai–Suichang Uplift and tectonic evolution of Zhejiang Province, southeast China. Ore Geology Reviews 12, 35–55.

Potma, W., Rovardi, M., Weinberg, R., 2003. Modelling deformation and fluid flow associated with the Wallaby Gold Deposit mineralizing event. Geological Society of Australia, Abstract Volume 72 (SGTSG Conference, Kalbarri, Western Australia, September 2003), 93.

Rockfield Software Limited, 2001. ELFEN User Manual, version 3.0. Swansea, U.K.

Schaubs, P.M., Zhao, C., 2002. Numerical models of gold-deposit formation in the Bendigo–Ballarat Zone, Victoria. Australian Journal of Earth Sciences 49, 1077–1096.

Sibson, R.H., 1994. Crustal stress, faulting and fluid flow. In: Parnell, J. (Ed.), Geofluids: Origin, Migration and Evolution of Fluids in Sedimentary Basins. Geological Society, London, Special Publication, vol. 78, pp. 69–84.

Sorjonen-Ward, P., Zhang, Y., Zhao, C., 2002. Numerical modeling of orogenic processes and gold mineralisation in the southeastern part of the Yilgarn craton, Western Australia. Australian Journal of Earth Sciences 49, 1011–1039.

Tao, K.Y., Mao, J.W., Xing, G.F., Yang, Z.L., Zhao, Y., 1999. Strong Yangshanian volcanic–magmatic explosion in east China. Mineral Deposits 18, 316–322 (in Chinese with an English abstract).

Turcotte, D.L., Schubert, G., 1982. Geodynamics: Applications of Continuum Physics to Geological Problems. Wiley, New York. 450 pp.

Vermeer, P.A., de Borst, R., 1984. Non-associated plasticity for soils, concrete and rock. Heron 29, 1–64.

Wang, Y.J., Fan, W.M., Guo, F., Li, H.M., Liang, X.Q., 2002a. U–Pb dating of early Mesozoic granodioritic intrusions in southeastern Hunan Provinces and its petrogenetic implications. Science in China, Series D: Earth Sciences 45, 280–288.

Wang, Y.J., Zhang, Y., Fan, W.M., Xi, X., Guo, F., Lin, G., 2002b. Numerical modelling of the formation of Indo-Sinian peraluminous granitoids Hunan Province: basaltic underplating versus tectonic thickening. Science in China, Series D: Earth Sciences 45, 1042–1056.

Wang, Y.J., Fan, W.M., Guo, F., 2003a. Geochemistry of early Mesozoic potassium-rich dioritic–granodioritic intrusions in Southeastern Hunan Province, South China: petrogenesis and tectonic implications. Geochemical Journal 37, 427–448.

Wang, Y.J., Fan, W.M., Guo, F., Peng, T.P., Li, C.W., 2003b. Geochemistry of Mesozoic mafic rocks around the Chenzhou–Linwu fault in South China: implication for the lithospheric boundary between the Yangtze and the Cathaysia Blocks. International Geology Review 45, 263–286.

Wang, Y.J., Fan, W.M., Peng, T.P., Guo, F., 2005. Element and Sr–Nd systematics of the early Mesozoic volcanic sequence in southern Jiangxi Province, South China: petrogenesis and tectonic implications. International Journal of Earth Sciences 94, 53–65.

Wu, X., 1994. Gold deposits and ductile shear zones. In: Song, B. (Ed.), New Developments in Research on Gold Deposits of China, volume 1-1, Chapter 6. Seismic Publishing House, Beijing, pp. 351–364 (in Chinese).

Yan, D.P., Zhou, M.F., Song, H.L., Wang, X.W., Malpas, J., 2003. Origin and tectonic significance of a Mesozoic multi-layer overthrust system within the Yangtze Bock (South China). Tectonophysics 361, 239–254.

Yang, K., 1996. Gold deposits in China: main types and potential. International Geology Review 38, 1006–1019.

Yin, A., Nie, S., 1993. An indentation model for the North and South China collision and the development of the Tan-Lu and Honam fault systems. Eastern Asia Tectonics, vol. 12, pp. 801–813.

Yu, H.X., Liu, J.Y., 1997. The granitic subvolcanic complex and polymetallic mineralisation in Shuikoushan orefield. Contributions to Geology and Mineral Resources Research 12, 35–44.

Zeng, N., Izawa, E., Motomura, Y., Lai, L., 2000. Silver minerals and paragenesis in the Kangjiawan Pb–Zn–Ag–Au deposit of the Shuikoushan mineral district, Hunan Province, China. Canadian Mineralogist 38, 11–22.

Zhai, Y., Deng, J., 1996. Outline of the mineral resources of China and their tectonic setting. Australian Journal of Earth Sciences 43, 673–685.

Zhang, Q.H., 1999. The geological characteristics of the Shuikoushan lead–zinc ore field in Hunan and the prospecting thought clues. Geological Exploration for Non-Ferrous Metals 8, 141–146 (in Chinese with English abstract).

Zhang, S., Cox, S.F., 2000. Enhancement of fluid permeability during shear deformation of a synthetic mud. Journal of Structural Geology 22, 795–806.

Zhang, Y., Hobbs, B.E., Ord, A., Mühlhaus, H.-B., 1996. Computer simulation of single layer buckling. Journal of Structural Geology 18, 643–655.

Zhang, S., Tullis, T.E., Scruggs, V.J., 1999. Permeability anisotropy and pressure dependence of permeability in experimentally sheared gouge materials. Journal of Structural Geology 21, 1385–1393.

Zhang, Y., Mancktelow, Neil, S., Hobbs, B.E., Ord, A., Mühlhaus, H.-B., 2000. Numerical modelling of single-layer folding: clarification of an issue regarding the effect of computer codes and the influence of initial irregularities. Journal of Structural Geology 22, 1511–1522.

Zhang, Y., Hobbs, B.E., Ord, A., Barnicoat, A., Zhao, C., Walshe, J.L., Lin, G., 2003. The influence of faulting on host-rock permeability, fluid flow and ore genesis of gold deposits: a theoretical 2D numerical model. Journal of Geochemical Exploration 78–79, 279–284.

Zhang, Y., Lin, G., Wang, Y.J., Roberts, P.A., Ord, A., 2004. Application of thermal-deformation-fluid flow modeling to mineral exploration in the Shuikoushan mineralisation district, Hunan Province, China. In: McPhie, J., McGoldrick, P. (Eds.), Dynamic Earth: Past, Present and Future, 17th Australian Geological Convention, 8–13 February, 2004. Geological Society of Australia Abstract, vol. 73, p. 140.

Zhou, T., Goldfarb, R.J., Phillips, G.N., 2002. Tectonics and distribution of gold deposits in China—an overview. Mineralium Deposita 37, 249–282.

Zhuang, J.L., Liu, Z.W., Tan, B.X., 1988. Relation of the small rock bodies in southern Hunan to the formation of ore deposits and prognosis of concealed deposits. Hunan Geology 4, 1–163 (supplement.) (in Chinese).